JOURNAL OF MATERIALS PROCESSING TECHNOLOGY 203 (2008) 561–562

ELSEVIER

available at www.sciencedirect.com

ScienceDirect

journal homepage: www.elsevier.com/locate/jmatprotec

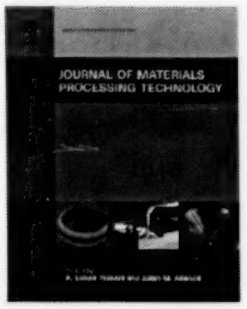

Author Index of Volume 203

Abachi, P., 554
Abouei, V., 107
Abrão, A.M., 431
Acselrad, O., 13
Aggarwal, R.K., 184
Ahn, B., 37
Akbarzadeh, A., 293
Aniolek, M., 333
Antonelli, E., 526
Arabi, H., 349
Artir, R., 465
Asgari, S.A., 129
Avci, E., 465
Ayedi, H.F., 404

Bacha, A., 480
Bache, M.R., 439
Bahrami, A., 554
Balasubramanian, K., 321
Baradai, C., 80
Barisic, B., 154
Bataller, R.C., 176
Bayramoglu, M., 277
Bigdeli Karimi, M., 349
Blignault, C., 46
Bortels, L., 58
Bortot, P., 381

Canteli, J.A., 267
Cantero, J.L., 267
Ceretti, E., 381
Cetlin, P.R., 13
Chandrasekar, S., 365
Chang, S.-H., 365
Chen, C., 202
Chen, J., 86
Chen, J.-C., 548
Chen, S.L., 461
Chen, X., 420
Chen, Y., 301
Chen, Y.-C., 117
Cheng, B., 449
Chi, Y., 548
Chiou, S.Y., 461
Choudhury, S.K., 95
Clark, D., 439
Clemente, V.C., 537
Correia, A.E., 431
Cui, J., 310
Cui, Z., 193

Dahotre, N.B., 498
Daneshi, G., 293
Daniel, D., 480
Dar, N.U., 193
Davim, J.P., 431, 537
de Souza, T., 1
de Vicente, F.S., 526
Deconinck, J., 58
Demirkiran, A.Ş., 465
Deng, D., 252
Deng, X.-X., 548
Dhakate, S.R., 184
Dhami, T.L., 184
Dingle, M., 129
Dorochenko, A., 58
Dutta Majumdar, J., 505

El Domiaty, A., 372
El Megharbel, A., 372
El Nasser, G.A., 372
Elhalouani, F., 80
Elleuch, K., 404
Elmustafa, A.A., 411
Emadoddin, E., 293
Erdmann, M., 19

Fang, H., 216
Farris, T.N., 365
Ferry, M., 518
Fu, Y.C., 166

Gaitonde, V.N., 431
Gao, L., 193
Ge, Y.F., 166
Geren, N., 277
Giardini, C., 381
Gindy, N., 420
Gordani, G.R., 315
Grujicic, M., 19
Guermazi, N., 404
Gupta, D.K., 184
Gupta, G.S., 471

Han, S., 117
Hasheminia, S., 113
Hattingh, D.G., 46
Hayat, N., 193
Hernandes, A.C., 526
Hocheng, H., 342
Hodgson, P.D., 129
Holzleitner, J., 19

Hsieh, C.-T., 326
Hsieh, S.F., 461
Huang, Z., 310
Hussain, G., 193

James, M.N., 46
Jeong, H., 287
Jesionowski, T., 121
Jeyakumar, M., 471
Joseph Davidson, M., 321

Kalyan Kumar, K.V.B.S., 95
Kannan, A.R., 542
Kapsa, P., 404
Karnik, S.R., 431
Kasprzak, W., 333
KhatibZadeh, S., 113
Kheirandish, S., 107
Khosravani, A., 349
Kim, H., 287
Kim, K.S., 232
Kiminami, R.H.G.A., 513
Klocker, H., 480
Ko, Y.-D., 454
Kumar, S., 471
Kurita, H., 333
Kurnia, W., 241
Kuroda, M., 396
Kweon, K.E., 454

Lajimi, A.M., 72
Lavernia, E.J., 37
Lee, H., 287
Lee, J.H., 454
Li, G., 19
Li, Z., 449
Liang, W., 252
Lin, M.H., 461
Liu, L., 548
Liu, Q., 420
Liu, X., 202
Liu, X.-K., 548
Lu, F., 301
Luo, S.B., 166

Madaah-Hosseini, H.R., 554
Mandal, S., 411
Manna, A., 147
Manna, I., 505
Marrow, T.J., 396
Math, M.D., 154

Elsevier B.V.
doi:10.1016/S0924-0136(08)00423-8

Mathur, R.B., 184
Menezes, R.R., 513
Miguélez, M.H., 267
Milad, M., 80
Miraghaei, S., 554
Monirvaghefi, M., 315
Moon, T.-H., 454
Moon, Y.H., 532
Murakawa, H., 252
Myoung, J.-M., 454

Nath, A.K., 505
Newbery, A.P., 37
Norasethasopon, S., 137
Novak, F., 208
Novak, S., 208
Nutt, S.R., 37

Ohdar, R.K., 102
Olofsson, D., 221
Onat, B., 277

Paital, S.R., 498
Pakshir, M., 389
Pandey, K.S., 542
Pandurangan, B., 19
Pang, Y.C., 193
Pao, P.S., 37
Park, B., 287
Park, K., 287
Pavlina, E.J., 532
Pepelnjak, T., 154
Pereira, I.M., 13
Pereira, M., 129
Purcar, M., 58

Rai, J.K., 72
Ramesh Chandra, B., 505
Ranjbar, K., 107
Razavi, R.S., 315
Rice, J., 411
Rolfe, B., 1
Rolfe, B.F., 129
Rubim, G., 13
Rubio, J.C., 431
Ryu, C., 232

Saghafian, H., 107
Salehi, M., 315
Salodkar, S., 147
Samant, A.N., 498
Samedani, M., 113
Samei, J., 349
Satish, G.D., 102
Sellappan, V., 19
Seyr, N., 19
Shahryari, A., 389
Shanmugam, S., 542
Shr, J.-F., 326
Silva, R.S., 526
Silva, S., 537
Singh, N.K., 102
Sokolowski, J.H., 333
Spuskanyuk, A., 305
Spuskanyuk, V., 305
Sun, D., 86

Tagore, G.R.N., 321
Tan, P.C., 241
Tang, Y., 548
Tasdelen, B., 221
Thordenberg, H., 221
Tong, L., 86
Tong, Z., 449
Topping, T.D., 37
Torkar, D., 208
Tsao, C.C., 342
Tzeng, Y.-f., 355

Vahidi, A., 19
Van den Bossche, B., 58
van Niekerk, T.I., 46
Van Tyne, C.J., 532
Varyukhin, V., 305

Wan, Z.-P., 548
Wang, D.-Y., 117
Wang, Y., 420
Wei, J., 86
Weng, K.-W., 117
Whittaker, M.T., 439
Wu, C.-F., 326
Wu, C.-H., 326

Xirouchakis, P., 72
Xu, J.H., 166
Xu, W., 216, 518

Yamagata, H., 333
Yang, H., 166
Yao, S., 301
Yekta, B.E., 113
Yeo, S.H., 241
Yi, H.K., 532
Yun, I., 454

Zanatta, A.R., 526
Zhang, R., 449
Zhang, Y., 202, 301
Zhao, H., 310
Zhao, L., 202
Zhou, W., 202
Zreiba, N., 80

JOURNAL OF MATERIALS PROCESSING TECHNOLOGY 203 (2008) 563–571

available at www.sciencedirect.com

ScienceDirect

journal homepage: www.elsevier.com/locate/jmatprotec

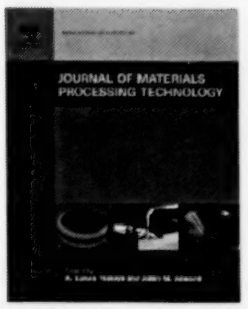

Subject Index of Volume 203

AA6061 alloy
An experimental study on the quality of flow-formed AA6061 tubes, 321
ABAQUS
Experimental and numerical investigation of the plunge stage in friction stir welding, 411
Acicular ferrite
Comparison of recrystallization behaviour of cold deformed acicular ferrite produced by conventional processing and direct strip casting, 518
Active resistance
Analysis of the variation regularity of the parameters of the discharge circuit with the distance between workpiece and inductor for electromagnetic forming processes, 216
Adhesion
Characteristics of diamond-like carbon film deposited by filter arc deposition, 117
Adsorptive properties
Synthesis and characterization of spherical silica precipitated via emulsion route, 121
Aerospace components
Shaped metal deposition of a nickel alloy for aero engine applications, 439
Aging impact
Aging effect on thermal, mechanical and tribological behaviour of polymeric coatings used for pipeline application, 404
Air
An experimental investigation on contact length during minimum quantity lubrication (MQL) machining, 221
Air bending
Experimental identification of a thermo-mechanical model for air bending, 267
Al–20% Si alloy
The effect of average cooling rates on the microstructure of the Al–20% Si high pressure die casting alloy used for monolithic cylinder blocks, 333
Alloy 718
Shaped metal deposition of a nickel alloy for aero engine applications, 439
Alumina
Process optimization in laser surface structuring of alumina, 498
Microwave sintering of alumina–zirconia nano composites, 513
Aluminum alloy tube
Application of a combined heating system for the warm hydroforming of lightweight alloy tubes, 532
Analysis of variance
Preparation of fatigue specimens with controlled surface characteristics, 396
ANN
An intelligent system for predicting HPDC process variables in interactive environment, 72
ANOVA
Analysis of parametric influence on delamination in high-speed drilling of carbon fiber reinforced plastic composites, 431
Area fraction
Influence of process parameters on shape quality and area fraction in round-to-hexagonal composite wire drawing, 137
Artificial neural networks
Apparent viscosity prediction of alumina–paraffin suspensions using artificial neural networks, 208
Aspiration pressure
Modeling of gas flow inside and outside the nozzle used in spray deposition, 471
Austenitic stainless steel
The effect of cold work on structure and properties of AISI 304 stainless steel, 80
Austenitic steel
Effect of rolling strain on transformation induced plasticity of austenite to martensite in a high-alloy austenitic steel, 349
Automatic mesh generation
Advanced and automatic determination of initial configuration of curved shell plates for flame bending, 232
Automotive structural components
Computational analysis of injection-molding residual-stress development in direct-adhesion polymer-to-metal hybrid body-in-white components, 19

Bamboo charcoals
Synthesis and photocatalytic characterization of titania-supported bamboo charcoals by using sol–gel method, 326
Barium calcium titanate
Electrophoretic deposition of $Ba_{0.77}Ca_{0.23}TiO_3$ nano powders, 526
Brazing technology parameter
Scanning electron beam brazing of thin-wall capillary tube–sheet structure, 301

CAD model reconstruction
Advanced CAD integrated approach for 3D electro-chemical machining simulations, 58

Elsevier B.V.
doi:10.1016/S0924-0136(08)00424-X

Calculation of pressure
Development of the equal-channel angular hydroextrusion, 305
Candle stick drill
Evaluation of thrust force and surface roughness in drilling composite material using Taguchi analysis and neural network, 342
Carbon black
Effect of different carbon fillers on the properties of graphite composite bipolar plate, 184
Carbon fiber reinforced plastics (CFRP)
Analysis of parametric influence on delamination in high-speed drilling of carbon fiber reinforced plastic composites, 431
Carbon fibers
Effect of different carbon fillers on the properties of graphite composite bipolar plate, 184
Ceramics
Apparent viscosity prediction of alumina–paraffin suspensions using artificial neural networks, 208
Process optimization in laser surface structuring of alumina, 498
Ceria slurry
Pad roughness variation and its effect on material removal profile in ceria-based CMP slurry, 287
Chemical composition
Effect of cold rolling reduction and intercritical annealing temperature on the bulk texture of two TRIP-aided steel sheets, 293
Chemical mechanical polishing
Pad roughness variation and its effect on material removal profile in ceria-based CMP slurry, 287
Chromium plating
Statistical optimization of process parameters to obtain maximum thickness and brightness in chromium plating, 277
Cladding
Studies on compositionally graded silicon carbide dispersed composite surface on mild steel developed by laser surface cladding, 505
Cold deformation
Some investigation on the cold deformation behaviour of sintered iron–0.8% carbon alloy powder preforms, 542
Cold rolled sheet
Effect of cold rolling reduction and intercritical annealing temperature on the bulk texture of two TRIP-aided steel sheets, 293
Cold rolling
The effect of cold work on structure and properties of AISI 304 stainless steel, 80
Combined heating
Application of a combined heating system for the warm hydroforming of lightweight alloy tubes, 532
Composite bipolar plate
Effect of different carbon fillers on the properties of graphite composite bipolar plate, 184
Composite material
Evaluation of thrust force and surface roughness in drilling composite material using Taguchi analysis and neural network, 342
Computer-aided design
Advanced CAD integrated approach for 3D electrochemical machining simulations, 58
Contact length
An experimental investigation on contact length during minimum quantity lubrication (MQL) machining, 221
Control
Scanning electron beam brazing of thin-wall capillary tube–sheet structure, 301
Convergent nozzle configurations
Modeling of gas flow inside and outside the nozzle used in spray deposition, 471
Copper film
A novel method of electroless plating on AZ31 magnesium alloy sheet, 310
Corrosion
A novel method of electroless plating on AZ31 magnesium alloy sheet, 310
Corrosion behaviour of laser gas-nitrided Ti–6Al–4V alloy in nitric acid solution, 315
Studies on compositionally graded silicon carbide dispersed composite surface on mild steel developed by laser surface cladding, 505
Cryogenic machining
Investigation of tool wear and cutting force in cryogenic machining using design of experiments, 95
Cutting depth
Preparation of fatigue specimens with controlled surface characteristics, 396
Cutting force
Investigation of tool wear and cutting force in cryogenic machining using design of experiments, 95
Cutting pipe mechanism
The characteristics of cutting pipe mechanism with multi-electrodes in EDM, 461
Cylinder block
The effect of average cooling rates on the microstructure of the Al–20% Si high pressure die casting alloy used for monolithic cylinder blocks, 333

3D FEM
Influence of process parameters on shape quality and area fraction in round-to-hexagonal composite wire drawing, 137
3D modelling
Advanced CAD integrated approach for 3D electrochemical machining simulations, 58
Decorating sphere
Precision control of explosive forming for metallic decorating sphere, 449
Degradation
Aging effect on thermal, mechanical and tribological behaviour of polymeric coatings used for pipeline application, 404
Delamination
Analysis of parametric influence on delamination in high-speed drilling of carbon fiber reinforced plastic composites, 431
Drilling investigation of MDF (medium density fibreboard), 537
Delamination wear
An investigation of the wear behaviour of 0.2% C dual phase steels, 107
Densification
Some investigation on the cold deformation behaviour of sintered iron–0.8% carbon alloy powder preforms, 542
Design of Experiment
Statistical analysis of finite element modeling in sheet metal forming and springback analysis, 129
Diamond turning
Workpiece surface quality when ultra-precision turning of SiC_p/Al composites, 166

Diamond-like carbon
Characteristics of diamond-like carbon film deposited by filter arc deposition, 117
Die design
Preform optimization of pad section of front axle beam using DEFORM, 102
Discharging current
Analysis of the variation regularity of the parameters of the discharge circuit with the distance between workpiece and inductor for electromagnetic forming processes, 216
Distance
Analysis of the variation regularity of the parameters of the discharge circuit with the distance between workpiece and inductor for electromagnetic forming processes, 216
Drawing stress
Influence of process parameters on shape quality and area fraction in round-to-hexagonal composite wire drawing, 137
Drilling
Evaluation of thrust force and surface roughness in drilling composite material using Taguchi analysis and neural network, 342
Drilling investigation of MDF (medium density fibreboard), 537
Dry
An experimental investigation on contact length during minimum quantity lubrication (MQL) machining, 221
Dual phase steel
An investigation of the wear behaviour of 0.2% C dual phase steels, 107
Ductile fracture
A novel finned micro-groove array structure and forming process, 548
Ductility
Metal ductility at low stress triaxiality application to sheet trimming, 480
Dynamic programming
Optimization of machining conditions for effective turning of E0300 alloy steel, 147

E0300 alloys steel
Optimization of machining conditions for effective turning of E0300 alloy steel, 147
EBSD
Comparison of recrystallization behaviour of cold deformed acicular ferrite produced by conventional processing and direct strip casting, 518
Effect of shape
Numerical investigation on multiphase coupling heat conduction with subcooling boiling boundary conditions and effect of shape during quenching process, 86
Elastic plastic material
Metal ductility at low stress triaxiality application to sheet trimming, 480
Electrical discharge machining
The characteristics of cutting pipe mechanism with multi-electrodes in EDM, 461
Electrical discharge machining (EDM)
Critical assessment and numerical comparison of electro-thermal models in EDM, 241
Development of a flexible high-speed EDM technology with geometrical transform optimization, 355
Electrical resistivity
Effect of different carbon fillers on the properties of graphite composite bipolar plate, 184
Electrochemical machining
Advanced CAD integrated approach for 3D electrochemical machining simulations, 58
Electrode shape change
Advanced CAD integrated approach for 3D electrochemical machining simulations, 58
Electroless plating
A novel method of electroless plating on AZ31 magnesium alloy sheet, 310
Electromagnetic field
Influence of a modulated electromagnetic field on fouling in a double-pipe heat exchanger, 389
Electrophoretic deposition
Electrophoretic deposition of $Ba_{0.77}Ca_{0.23}TiO_3$ nanopowders, 526
Electro-thermal model
Critical assessment and numerical comparison of electro-thermal models in EDM, 241
Elovich kinetic model
Synthesis and photocatalytic characterization of titania-supported bamboo charcoals by using sol–gel method, 326
Emulsion
Synthesis and characterization of spherical silica precipitated via emulsion route, 121
Energy dispersive spectroscopy
Experimental and numerical investigation of the plunge stage in friction stir welding, 411
Equal-channel angular extrusion
Development of the equal-channel angular hydroextrusion, 305
Equivalent inductance
Analysis of the variation regularity of the parameters of the discharge circuit with the distance between workpiece and inductor for electromagnetic forming processes, 216
Evolution
Experimental analysis on evolution of superfinished surface texture, 365
Explosive forming
Precision control of explosive forming for metallic decorating sphere, 449
Extrusion
Large UFG Al alloy plates from cryomilling, 37
A novel finned micro-groove array structure and forming process, 548

FE simulations
The determination of flow stress of tubular material for hydroforming applications, 381
Feed rate
Preparation of fatigue specimens with controlled surface characteristics, 396
Ferroelectric
Electrophoretic deposition of $Ba_{0.77}Ca_{0.23}TiO_3$ nanopowders, 526
Ferromagnetic
The effect of cold work on structure and properties of AISI 304 stainless steel, 80
Filling time
An intelligent system for predicting HPDC process variables in interactive environment, 72
Filter arc deposition
Characteristics of diamond-like carbon film deposited by filter arc deposition, 117

Finite element analysis
Comparison of the experimental and the numerically predicted mechanical damage in the sheet forming of steel, 13
Finite element method
Advanced CAD integrated approach for 3D electrochemical machining simulations, 58
Prediction of welding distortion in a curved plate structure by means of elastic finite element method, 252
Finite elements
Advanced and automatic determination of initial configuration of curved shell plates for flame bending, 232
Metal ductility at low stress triaxiality application to sheet trimming, 480
Finned surface
A novel finned micro-groove array structure and forming process, 548
Flow-forming
An experimental study on the quality of flow-formed AA6061 tubes, 321
Fluor-phlogopite
Effect of sintering and melt casting methods on properties of a machinable fluor-phlogopite glass–ceramic, 113
Force footprint
Characterization of the influences of FSW tool geometry on welding forces and weld tensile strength using an instrumented tool, 46
Force monitoring
Characterization of the influences of FSW tool geometry on welding forces and weld tensile strength using an instrumented tool, 46
Forming limit
Some investigation on the cold deformation behaviour of sintered iron–0.8% carbon alloy powder preforms, 542
Fouling
Influence of a modulated electromagnetic field on fouling in a double-pipe heat exchanger, 389
Fracture mechanisms
Metal ductility at low stress triaxiality application to sheet trimming, 480
Friction
Development of the equal-channel angular hydroextrusion, 305
Friction stir welding
Characterization of the influences of FSW tool geometry on welding forces and weld tensile strength using an instrumented tool, 46
Front axle beam
Preform optimization of pad section of front axle beam using DEFORM, 102
FSW
Experimental and numerical investigation of the plunge stage in friction stir welding, 411

Gap
Prediction of welding distortion in a curved plate structure by means of elastic finite element method, 252
Gas atomization
Modeling of gas flow inside and outside the nozzle used in spray deposition, 471
Grinding force modelling
Empirical modelling of grinding force based on multivariate analysis, 420

Hardness
Effect of rolling strain on transformation induced plasticity of austenite to martensite in a high-alloy austenitic steel, 349
Heat conduction
Numerical investigation on multiphase coupling heat conduction with subcooling boiling boundary conditions and effect of shape during quenching process, 86
Heat transfer
Influence of a modulated electromagnetic field on fouling in a double-pipe heat exchanger, 389
Heat treatment
An investigation of the wear behaviour of 0.2% C dual phase steels, 107
Heating element
Application of a combined heating system for the warm hydroforming of lightweight alloy tubes, 532
Hexagonal composite wire
Influence of process parameters on shape quality and area fraction in round-to-hexagonal composite wire drawing, 137
HfO_2
Statistical modeling of the electrical characteristics for HfO_2 thin films grown by MOMBE for high-k dielectric applications, 454
High pressure die casting
The effect of average cooling rates on the microstructure of the Al–20% Si high pressure die casting alloy used for monolithic cylinder blocks, 333
High temperature
Experimental identification of a thermo-mechanical model for air bending, 267
High-speed drilling
Analysis of parametric influence on delamination in high-speed drilling of carbon fiber reinforced plastic composites, 431
Hot isostatic pressing
Large UFG Al alloy plates from cryomilling, 37
HPDC
An intelligent system for predicting HPDC process variables in interactive environment, 72
Hydroextrusion
Development of the equal-channel angular hydroextrusion, 305
Hygrothermal aging
Aging effect on thermal, mechanical and tribological behaviour of polymeric coatings used for pipeline application, 404

Ideal function
Development of a flexible high-speed EDM technology with geometrical transform optimization, 355
Induction heating
Application of a combined heating system for the warm hydroforming of lightweight alloy tubes, 532
Inherent deformation
Prediction of welding distortion in a curved plate structure by means of elastic finite element method, 252
Instrumented tool
Characterization of the influences of FSW tool geometry on welding forces and weld tensile strength using an instrumented tool, 46
Intercritical annealing
Effect of cold rolling reduction and intercritical annealing temperature on the bulk texture of two TRIP-aided steel sheets, 293

Interface element
Prediction of welding distortion in a curved plate structure by means of elastic finite element method, 252
Interlayer
A novel method of electroless plating on AZ31 magnesium alloy sheet, 310

Johnson–Cook law
Experimental and numerical investigation of the plunge stage in friction stir welding, 411

Laminar boundary layer
Similarity solutions for flow and heat transfer of a quiescent fluid over a nonlinearly stretching surface, 176
Laplace equation
Advanced CAD integrated approach for 3D electrochemical machining simulations, 58
Laser
Studies on compositionally graded silicon carbide dispersed composite surface on mild steel developed by laser surface cladding, 505
Laser gas nitriding
Corrosion behaviour of laser gas-nitrided Ti–6Al–4V alloy in nitric acid solution, 315
Lüders' bands (stretcher strains)
Predicting of the Lüders' bands in the processing of TH material in computer environment by means of stochastic modeling, 154
Low carbon steel
Comparison of recrystallization behaviour of cold deformed acicular ferrite produced by conventional processing and direct strip casting, 518
Low-pressure injection moulding
Apparent viscosity prediction of alumina–paraffin suspensions using artificial neural networks, 208
Lubricant
Tool and lubrication for negative incremental forming of a commercially pure titanium sheet, 193
Lubrication method
Tool and lubrication for negative incremental forming of a commercially pure titanium sheet, 193

Magnetic measurement
Effect of rolling strain on transformation induced plasticity of austenite to martensite in a high-alloy austenitic steel, 349
Marciniak test
Comparison of the experimental and the numerically predicted mechanical damage in the sheet forming of steel, 13
Martensitic transformation
The effect of cold work on structure and properties of AISI 304 stainless steel, 80
Material removal
Pad roughness variation and its effect on material removal profile in ceria-based CMP slurry, 287
Material removal rate
The characteristics of cutting pipe mechanism with multi-electrodes in EDM, 461
Mechanical alloying
Characterization of mechanically alloyed $Fe_{100-x}Si_x$ and $Fe_{83.5}Si_{13.5}Nb_3$ nanocrystalline powders, 554
Mechanical damage
Comparison of the experimental and the numerically predicted mechanical damage in the sheet forming of steel, 13
Mechanical properties
Large UFG Al alloy plates from cryomilling, 37
Effect of different carbon fillers on the properties of graphite composite bipolar plate, 184
Aging effect on thermal, mechanical and tribological behaviour of polymeric coatings used for pipeline application, 404
Medium density fibreboard (MDF)
Drilling investigation of MDF (medium density fibreboard), 537
Melt casting
Effect of sintering and melt casting methods on properties of a machinable fluor-phlogopite glass–ceramic, 113
Methylene blue
Synthesis and photocatalytic characterization of titania-supported bamboo charcoals by using sol–gel method, 326
Micro-groove
A novel finned micro-groove array structure and forming process, 548
Microstructure
An investigation of the wear behaviour of 0.2% C dual phase steels, 107
The effect of average cooling rates on the microstructure of the Al–20% Si high pressure die casting alloy used for monolithic cylinder blocks, 333
Shaped metal deposition of a nickel alloy for aero engine applications, 439
Microwave processing
Microwave sintering of alumina–zirconia nano-composites, 513
Mild steel
Studies on compositionally graded silicon carbide dispersed composite surface on mild steel developed by laser surface cladding, 505
Modeling of gas flow
Modeling of gas flow inside and outside the nozzle used in spray deposition, 471
Modelling
Experimental identification of a thermo-mechanical model for air bending, 267
Molecular dynamics
Study of ultrashort laser ablation of metals by molecular dynamics simulation and experimental method, 202
MOMBE
Statistical modeling of the electrical characteristics for HfO_2 thin films grown by MOMBE for high-k dielectric applications, 454
Monocrystalline copper
Study of ultrashort laser ablation of metals by molecular dynamics simulation and experimental method, 202
Moving cathode tools
Advanced CAD integrated approach for 3D electrochemical machining simulations, 58
MQL
An experimental investigation on contact length during minimum quantity lubrication (MQL) machining, 221
Multivariate regression
Empirical modelling of grinding force based on multivariate analysis, 420

Nanocomposite
Microwave sintering of alumina–zirconia nano-composites, 513

Nanocrystalline powder
Large UFG Al alloy plates from cryomilling, 37
Nanostructured Fe–Si powder
Characterization of mechanically alloyed $Fe_{100-x}Si_x$ and $Fe_{83.5}Si_{13.5}Nb_3$ nanocrystalline powders, 554
Natural graphite
Effect of different carbon fillers on the properties of graphite composite bipolar plate, 184
Nd:YAG laser
Process optimization in laser surface structuring of alumina, 498
Negative incremental forming
Tool and lubrication for negative incremental forming of a commercially pure titanium sheet, 193
Nonlinear deformation theory
Advanced and automatic determination of initial configuration of curved shell plates for flame bending, 232
Nonlinearly stretching surfaces
Similarity solutions for flow and heat transfer of a quiescent fluid over a nonlinearly stretching surface, 176

Optimal surface development
Advanced and automatic determination of initial configuration of curved shell plates for flame bending, 232
Optimization
Development of a flexible high-speed EDM technology with geometrical transform optimization, 355
Process optimization in laser surface structuring of alumina, 498
Optimized cost
Optimization of machining conditions for effective turning of E0300 alloy steel, 147
Optimum filter selection
Empirical modelling of grinding force based on multivariate analysis, 420
Organic coating
A novel method of electroless plating on AZ31 magnesium alloy sheet, 310

Pad roughness
Pad roughness variation and its effect on material removal profile in ceria-based CMP slurry, 287
Pad section
Preform optimization of pad section of front axle beam using DEFORM, 102
Particle reinforced aluminum matrix composites
Workpiece surface quality when ultra-precision turning of SiC_p/Al composites, 166
Particle size distribution and surface morphology
Synthesis and characterization of spherical silica precipitated via emulsion route, 121
Phase transformation
Numerical investigation on multiphase coupling heat conduction with subcooling boiling boundary conditions and effect of shape during quenching process, 86
Photocatalysis
Synthesis and photocatalytic characterization of titania-supported bamboo charcoals by using sol–gel method, 326
Plating brightness
Statistical optimization of process parameters to obtain maximum thickness and brightness in chromium plating, 277
Plating thickness
Statistical optimization of process parameters to obtain maximum thickness and brightness in chromium plating, 277
Ploughing
A novel finned micro-groove array structure and forming process, 548
Plunge
Experimental and numerical investigation of the plunge stage in friction stir welding, 411
Poisson's ratio
Some investigation on the cold deformation behaviour of sintered iron–0.8% carbon alloy powder preforms, 542
Polymer metal hybrids
Computational analysis of injection-molding residual-stress development in direct-adhesion polymer-to-metal hybrid body-in-white components, 19
Polymeric coatings
Aging effect on thermal, mechanical and tribological behaviour of polymeric coatings used for pipeline application, 404
Porcelain
Effect of natural zeolite addition on sintering kinetics of porcelain bodies, 465
Porosity
An intelligent system for predicting HPDC process variables in interactive environment, 72
Precipitation
Synthesis and characterization of spherical silica precipitated via emulsion route, 121
Precision control
Precision control of explosive forming for metallic decorating sphere, 449
Preform
Preform optimization of pad section of front axle beam using DEFORM, 102
Primary silicon
The effect of average cooling rates on the microstructure of the Al–20% Si high pressure die casting alloy used for monolithic cylinder blocks, 333
Probabilistic modelling
Multivariate modelling of variability in sheet metal forming, 1
Process modeling
Statistical modeling of the electrical characteristics for HfO_2 thin films grown by MOMBE for high-k dielectric applications, 454
Process optimisation
Characterization of the influences of FSW tool geometry on welding forces and weld tensile strength using an instrumented tool, 46
Protrusion length
Modeling of gas flow inside and outside the nozzle used in spray deposition, 471

Quality issues
An experimental study on the quality of flow-formed AA6061 tubes, 321
Quasi-isostatic forging
Large UFG Al alloy plates from cryomilling, 37
Quenching
Numerical investigation on multiphase coupling heat conduction with subcooling boiling boundary conditions and effect of shape during quenching process, 86

Radial basis function network
Evaluation of thrust force and surface roughness in drilling composite material using Taguchi analysis and neural network, 342
Rapid solidification
The effect of average cooling rates on the microstructure of the Al–20% Si high pressure die casting alloy used for monolithic cylinder blocks, 333
Reaction efficiency
Advanced CAD integrated approach for 3D electrochemical machining simulations, 58
Recrystallization
Comparison of recrystallization behaviour of cold deformed acicular ferrite produced by conventional processing and direct strip casting, 518
Regression model
Statistical modeling of the electrical characteristics for HfO_2 thin films grown by MOMBE for high-k dielectric applications, 454
Relative electrode wear rate
The characteristics of cutting pipe mechanism with multi-electrodes in EDM, 461
Residual stresses
Computational analysis of injection-molding residual-stress development in direct-adhesion polymer-to-metal hybrid body-in-white components, 19
Characteristics of diamond-like carbon film deposited by filter arc deposition, 117
Bending of tube and section made of strain-hardening materials, 372
Preparation of fatigue specimens with controlled surface characteristics, 396
Response surface methodology
Preparation of fatigue specimens with controlled surface characteristics, 396
Analysis of parametric influence on delamination in high-speed drilling of carbon fiber reinforced plastic composites, 431
Robustness
Multivariate modelling of variability in sheet metal forming, 1
Rolling strain
Effect of rolling strain on transformation induced plasticity of austenite to martensite in a high-alloy austenitic steel, 349

Scanning electron beam
Scanning electron beam brazing of thin-wall capillary tube–sheet structure, 301
Seizure
An experimental investigation on contact length during minimum quantity lubrication (MQL) machining, 221
Shape quality
Influence of process parameters on shape quality and area fraction in round-to-hexagonal composite wire drawing, 137
Shaped metal deposition (SMD)
Shaped metal deposition of a nickel alloy for aero engine applications, 439
Sheet forming
Comparison of the experimental and the numerically predicted mechanical damage in the sheet forming of steel, 13
Sheet metal forming
Multivariate modelling of variability in sheet metal forming, 1
Experimental identification of a thermo-mechanical model for air bending, 267
SiC
Studies on compositionally graded silicon carbide dispersed composite surface on mild steel developed by laser surface cladding, 505
Simulation
Preform optimization of pad section of front axle beam using DEFORM, 102
Prediction of welding distortion in a curved plate structure by means of elastic finite element method, 252
Sinterability
Effect of sintering and melt casting methods on properties of a machinable fluor-phlogopite glass–ceramic, 113
Sintering
Microwave sintering of alumina–zirconia nano-composites, 513
Sintering activation energy
Effect of natural zeolite addition on sintering kinetics of porcelain bodies, 465
Sintering kinetics
Effect of natural zeolite addition on sintering kinetics of porcelain bodies, 465
Sliding
An experimental investigation on contact length during minimum quantity lubrication (MQL) machining, 221
Soft magnetic properties
Characterization of mechanically alloyed $Fe_{100-x}Si_x$ and $Fe_{83.5}Si_{13.5}Nb_3$ nanocrystalline powders, 554
Solidification time
An intelligent system for predicting HPDC process variables in interactive environment, 72
Spherical silica
Synthesis and characterization of spherical silica precipitated via emulsion route, 121
Springback
Multivariate modelling of variability in sheet metal forming, 1
Statistical analysis of finite element modeling in sheet metal forming and springback analysis, 129
Experimental identification of a thermo-mechanical model for air bending, 267
Bending of tube and section made of strain-hardening materials, 372
Statistical analysis
Statistical modeling of the electrical characteristics for HfO_2 thin films grown by MOMBE for high-k dielectric applications, 454
Statistical design
Statistical optimization of process parameters to obtain maximum thickness and brightness in chromium plating, 277
Steel sheets
Comparison of the experimental and the numerically predicted mechanical damage in the sheet forming of steel, 13
Stochastic modeling
Predicting of the Lüders' bands in the processing of TH material in computer environment by means of stochastic modeling, 154
Strip casting
Comparison of recrystallization behaviour of cold deformed acicular ferrite produced by conventional processing and direct strip casting, 518

Subcooling boiling heat transfer
Numerical investigation on multiphase coupling heat conduction with subcooling boiling boundary conditions and effect of shape during quenching process, 86
Superconductor
Influence of process parameters on shape quality and area fraction in round-to-hexagonal composite wire drawing, 137
Superfinishing
Experimental analysis on evolution of superfinished surface texture, 365
Surface
Studies on compositionally graded silicon carbide dispersed composite surface on mild steel developed by laser surface cladding, 505
Surface quality
Workpiece surface quality when ultra-precision turning of SiC_p/Al composites, 166
Tool and lubrication for negative incremental forming of a commercially pure titanium sheet, 193
Surface roughness
Evaluation of thrust force and surface roughness in drilling composite material using Taguchi analysis and neural network, 342
Preparation of fatigue specimens with controlled surface characteristics, 396
Surface texture
Experimental analysis on evolution of superfinished surface texture, 365

Taguchi method
Optimization of machining conditions for effective turning of E0300 alloy steel, 147
Evaluation of thrust force and surface roughness in drilling composite material using Taguchi analysis and neural network, 342
Process optimization in laser surface structuring of alumina, 498
Taguchi methods
Development of a flexible high-speed EDM technology with geometrical transform optimization, 355
Texture
Effect of cold rolling reduction and intercritical annealing temperature on the bulk texture of two TRIP-aided steel sheets, 293
Thermal radiation
Similarity solutions for flow and heat transfer of a quiescent fluid over a nonlinearly stretching surface, 176
Thick films
Electrophoretic deposition of $Ba_{0.77}Ca_{0.23}TiO_3$ nanopowders, 526
Thrust force
Evaluation of thrust force and surface roughness in drilling composite material using Taguchi analysis and neural network, 342
Ti–6Al–4V
Corrosion behaviour of laser gas-nitrided Ti–6Al–4V alloy in nitric acid solution, 315
Tinplate processing
Predicting of the Lüders' bands in the processing of TH material in computer environment by means of stochastic modeling, 154
Titania
Synthesis and photocatalytic characterization of titania-supported bamboo charcoals by using sol–gel method, 326
Tool
Tool and lubrication for negative incremental forming of a commercially pure titanium sheet, 193
Tool design
Characterization of the influences of FSW tool geometry on welding forces and weld tensile strength using an instrumented tool, 46
Tool life
Optimization of machining conditions for effective turning of E0300 alloy steel, 147
Tool torque
Characterization of the influences of FSW tool geometry on welding forces and weld tensile strength using an instrumented tool, 46
Tool wear
Investigation of tool wear and cutting force in cryogenic machining using design of experiments, 95
Transformation induced plasticity (TRIP)
Effect of rolling strain on transformation induced plasticity of austenite to martensite in a high-alloy austenitic steel, 349
TRIP steel
Statistical analysis of finite element modeling in sheet metal forming and springback analysis, 129
TRIP-aided steel
Effect of cold rolling reduction and intercritical annealing temperature on the bulk texture of two TRIP-aided steel sheets, 293
Tube bending
Bending of tube and section made of strain-hardening materials, 372
Tube bulge test
The determination of flow stress of tubular material for hydroforming applications, 381
Tube hydroforming
The determination of flow stress of tubular material for hydroforming applications, 381
Tube–sheet structure
Scanning electron beam brazing of thin-wall capillary tube–sheet structure, 301
Turning
Investigation of tool wear and cutting force in cryogenic machining using design of experiments, 95

Ultra-fine grained microstructure
Large UFG Al alloy plates from cryomilling, 37
Ultra-precision
Workpiece surface quality when ultra-precision turning of SiC_p/Al composites, 166
Ultrashort laser ablation
Study of ultrashort laser ablation of metals by molecular dynamics simulation and experimental method, 202
Ultra-thin wall
Precision control of explosive forming for metallic decorating sphere, 449

Variation
Multivariate modelling of variability in sheet metal forming, 1
Viscosity prediction
Apparent viscosity prediction of alumina–paraffin suspensions using artificial neural networks, 208
Viscous dissipation
Similarity solutions for flow and heat transfer of a quiescent fluid over a nonlinearly stretching surface, 176

Warm hydroforming
Application of a combined heating system for the warm hydroforming of lightweight alloy tubes, 532
Warpage
Computational analysis of injection-molding residual-stress development in direct-adhesion polymer-to-metal hybrid body-in-white components, 19
Water treatment
Influence of a modulated electromagnetic field on fouling in a double-pipe heat exchanger, 389
Wear
Studies on compositionally graded silicon carbide dispersed composite surface on mild steel developed by laser surface cladding, 505
Wear resistance
Aging effect on thermal, mechanical and tribological behaviour of polymeric coatings used for pipeline application, 404
Welding distortion
Prediction of welding distortion in a curved plate structure by means of elastic finite element method, 252

Zeolite
Effect of natural zeolite addition on sintering kinetics of porcelain bodies, 465
Zirconia
Microwave sintering of alumina–zirconia nano-composites, 513

ELSEVIER

Volume 203, Issues 1–3, 18 July 2008

Journal of
Materials
Processing
Technology

www.elsevier.com/locate/jmatprotec

Contents

Multivariate modelling of variability in sheet metal forming 1
T. de Souza, B. Rolfe

Comparison of the experimental and the numerically predicted mechanical damage in the sheet forming of steel 13
I.M. Pereira, G. Rubim, O. Acselrad, P.R. Cetlin

Computational analysis of injection-molding residual-stress development in direct-adhesion polymer-to-metal hybrid body-in-white components 19
M. Grujicic, V. Sellappan, B. Pandurangan, G. Li, A. Vahidi, N. Seyr, M. Erdmann, J. Holzleitner

Large UFG Al alloy plates from cryomilling 37
A.P. Newbery, B. Ahn, T.D. Topping, P.S. Pao, S.R. Nutt, E.J. Lavernia

Characterization of the influences of FSW tool geometry on welding forces and weld tensile strength using an instrumented tool 46
D.G. Hattingh, C. Blignault, T.I. van Niekerk, M.N. James

Advanced CAD integrated approach for 3D electrochemical machining simulations 58
M. Purcar, A. Dorochenko, L. Bortels, J. Deconinck, B. Van den Bossche

An intelligent system for predicting HPDC process variables in interactive environment 72
J.K. Rai, A.M. Lajimi, P. Xirouchakis

The effect of cold work on structure and properties of AISI 304 stainless steel 80
M. Milad, N. Zreiba, F. Elhalouani, C. Baradai

Numerical investigation on multiphase coupling heat conduction with subcooling boiling boundary conditions and effect of shape during quenching process 86
J. Chen, L. Tong, J. Wei, D. Sun

Investigation of tool wear and cutting force in cryogenic machining using design of experiments 95
K.V.B.S. Kalyan Kumar, S.K. Choudhury

Preform optimization of pad section of front axle beam using DEFORM 102
G.D. Satish, N.K. Singh, R.K. Ohdar

An investigation of the wear behaviour of 0.2% C dual phase steels 107
V. Abouei, H. Saghafian, S. Kheirandish, K. Ranjbar

Effect of sintering and melt casting methods on properties of a machinable fluor-phlogopite glass–ceramic 113
S. KhatibZadeh, M. Samedani, B.E. Yekta, S. Hasheminia

Characteristics of diamond-like carbon film deposited by filter arc deposition 117
K.-W. Weng, S. Han, Y.-C. Chen, D.-Y. Wang

Synthesis and characterization of spherical silica precipitated via emulsion route 121
T. Jesionowski

Statistical analysis of finite element modeling in sheet metal forming and springback analysis 129
S.A. Asgari, M. Pereira, B.F. Rolfe, M. Dingle, P.D. Hodgson

Influence of process parameters on shape quality and area fraction in round-to-hexagonal composite wire drawing 137
S. Norasethasopon

(Contents continued on page I)

0924-0136(20080718)203:1/3;1-8

(Contents continued from OBC)

Optimization of machining conditions for effective turning of E0300 alloy steel 147
A. Manna, S. Salodkar

Predicting of the Lüders' bands in the processing of TH material in computer environment by means of stochastic modeling 154
B. Barisic, T. Pepelnjak, M.D. Math

Workpiece surface quality when ultra-precision turning of SiC_p/Al composites 166
Y.F. Ge, J.H. Xu, H. Yang, S.B. Luo, Y.C. Fu

Similarity solutions for flow and heat transfer of a quiescent fluid over a nonlinearly stretching surface 176
R.C. Bataller

Effect of different carbon fillers on the properties of graphite composite bipolar plate 184
R.B. Mathur, S.R. Dhakate, D.K. Gupta, T.L. Dhami, R.K. Aggarwal

Tool and lubrication for negative incremental forming of a commercially pure titanium sheet 193
G. Hussain, L. Gao, N. Hayat, Z. Cui, Y.C. Pang, N.U. Dar

Study of ultrashort laser ablation of metals by molecular dynamics simulation and experimental method.... 202
X. Liu, W. Zhou, C. Chen, L. Zhao, Y. Zhang

Apparent viscosity prediction of alumina–paraffin suspensions using artificial neural networks 208
D. Torkar, S. Novak, F. Novak

Analysis of the variation regularity of the parameters of the discharge circuit with the distance between workpiece and inductor for electromagnetic forming processes 216
W. Xu, H. Fang, W. Xu

An experimental investigation on contact length during minimum quantity lubrication (MQL) machining.... 221
B. Tasdelen, H. Thordenberg, D. Olofsson

Advanced and automatic determination of initial configuration of curved shell plates for flame bending.... 232
C. Ryu, K.S. Kim

Critical assessment and numerical comparison of electro-thermal models in EDM 241
S.H. Yeo, W. Kurnia, P.C. Tan

Prediction of welding distortion in a curved plate structure by means of elastic finite element method 252
D. Deng, H. Murakawa, W. Liang

Experimental identification of a thermo-mechanical model for air bending 267
J.A. Canteli, J.L. Cantero, M.H. Miguélez

Statistical optimization of process parameters to obtain maximum thickness and brightness in chromium plating 277
M. Bayramoglu, B. Onat, N. Geren

Pad roughness variation and its effect on material removal profile in ceria-based CMP slurry..... 287
B. Park, H. Lee, K. Park, H. Kim, H. Jeong

Effect of cold rolling reduction and intercritical annealing temperature on the bulk texture of two TRIP-aided steel sheets 293
E. Emadoddin, A. Akbarzadeh, G. Daneshi

Scanning electron beam brazing of thin-wall capillary tube–sheet structure 301
Y. Chen, Y. Zhang, S. Yao, F. Lu

Development of the equal-channel angular hydroextrusion 305
V. Spuskanyuk, A. Spuskanyuk, V. Varyukhin

A novel method of electroless plating on AZ31 magnesium alloy sheet 310
H. Zhao, Z. Huang, J. Cui

Corrosion behaviour of laser gas-nitrided Ti–6Al–4V alloy in nitric acid solution..... 315
R.S. Razavi, M. Salehi, M. Monirvaghefi, G.R. Gordani

An experimental study on the quality of flow-formed AA6061 tubes..... 321
M. Joseph Davidson, K. Balasubramanian, G.R.N. Tagore

Synthesis and photocatalytic characterization of titania-supported bamboo charcoals by using sol–gel method..... 326
C.-H. Wu, J.-F. Shr, C.-F. Wu, C.-T. Hsieh

The effect of average cooling rates on the microstructure of the Al–20% Si high pressure die casting alloy used for monolithic cylinder blocks 333
H. Yamagata, W. Kasprzak, M. Aniolek, H. Kurita, J.H. Sokolowski

Evaluation of thrust force and surface roughness in drilling composite material using Taguchi analysis and neural network 342
C.C. Tsao, H. Hocheng

Effect of rolling strain on transformation induced plasticity of austenite to martensite in a high-alloy austenitic steel 349
M. Bigdeli Karimi, H. Arabi, A. Khosravani, J. Samei

Development of a flexible high-speed EDM technology with geometrical transform optimization 355
Y.-f. Tzeng

Experimental analysis on evolution of superfinished surface texture 365
S.-H. Chang, T.N. Farris, S. Chandrasekar

Bending of tube and section made of strain-hardening materials 372
A. El Megharbel, G.A. El Nasser, A. El Domiaty

The determination of flow stress of tubular material for hydroforming applications 381
P. Bortot, E. Ceretti, C. Giardini

Influence of a modulated electromagnetic field on fouling in a double-pipe heat exchanger 389
A. Shahryari, M. Pakshir

Preparation of fatigue specimens with controlled surface characteristics 396
M. Kuroda, T.J. Marrow

Aging effect on thermal, mechanical and tribological behaviour of polymeric coatings used for pipeline application 404
N. Guermazi, K. Elleuch, H.F. Ayedi, P. Kapsa

Experimental and numerical investigation of the plunge stage in friction stir welding 411
S. Mandal, J. Rice, A.A. Elmustafa

Empirical modelling of grinding force based on multivariate analysis 420
Q. Liu, X. Chen, Y. Wang, N. Gindy

Analysis of parametric influence on delamination in high-speed drilling of carbon fiber reinforced plastic composites 431
V.N. Gaitonde, S.R. Karnik, J.C. Rubio, A.E. Correia, A.M. Abrão, J.P. Davim

Shaped metal deposition of a nickel alloy for aero engine applications 439
D. Clark, M.R. Bache, M.T. Whittaker

Precision control of explosive forming for metallic decorating sphere 449
Z. Tong, Z. Li, B. Cheng, R. Zhang

Statistical modeling of the electrical characteristics for HfO_2 thin films grown by MOMBE for high-k dielectric applications 454
J.H. Lee, K.E. Kweon, Y.-D. Ko, T.-H. Moon, J.-M. Myoung, I. Yun

The characteristics of cutting pipe mechanism with multi-electrodes in EDM 461
S.L. Chen, M.H. Lin, S.F. Hsieh, S.Y. Chiou

Effect of natural zeolite addition on sintering kinetics of porcelain bodies 465
A.Ş. Demirkiran, R. Artir, E. Avci

Modeling of gas flow inside and outside the nozzle used in spray deposition 471
M. Jeyakumar, G.S. Gupta, S. Kumar

Metal ductility at low stress triaxiality application to sheet trimming 480
A. Bacha, D. Daniel, H. Klocker

Process optimization in laser surface structuring of alumina 498
A.N. Samant, S.R. Paital, N.B. Dahotre

Studies on compositionally graded silicon carbide dispersed composite surface on mild steel developed by laser surface cladding 505
J. Dutta Majumdar, B. Ramesh Chandra, A.K. Nath, I. Manna

Microwave sintering of alumina–zirconia nanocomposites 513
R.R. Menezes, R.H.G.A. Kiminami

Comparison of recrystallization behaviour of cold deformed acicular ferrite produced by conventional processing and direct strip casting 518
W. Xu, M. Ferry

Electrophoretic deposition of $Ba_{0.77}Ca_{0.23}TiO_3$ nanopowders 526
E. Antonelli, R.S. Silva, F.S. de Vicente, A.R. Zanatta, A.C. Hernandes

Application of a combined heating system for the warm hydroforming of lightweight alloy tubes 532
H.K. Yi, E.J. Pavlina, C.J. Van Tyne, Y.H. Moon

Drilling investigation of MDF (medium density fibreboard) 537
J.P. Davim, V.C. Clemente, S. Silva

Some investigation on the cold deformation behaviour of sintered iron–0.8% carbon alloy powder preforms ... 542
A.R. Kannan, K.S. Pandey, S. Shanmugam

A novel finned micro-groove array structure and forming process 548
Y. Tang, Y. Chi, Z.-P. Wan, X.-K. Liu, J.-C. Chen, X.-X. Deng, L. Liu

Characterization of mechanically alloyed $Fe_{100-x}Si_x$ and $Fe_{83.5}Si_{13.5}Nb_3$ nanocrystalline powders 554
S. Miraghaei, P. Abachi, H.R. Madaah-Hosseini, A. Bahrami

Author index 561

Subject index 563